Indonesian Physical Review
Volume 09 Issue 02, May 2026
P-ISSN: 2615-1278, E-ISSN: 2614-7904

Characterization of Green-Synthesized Cobalt Oxide Nanoparticles Using *Nigella sativa* Seed Extract

Hizkia Alpha Dewanto[1*], Sarah Toding[1], Irfan Riadin[1], Jatmoko Awali[1], Andi Idhil Ismail[2], Fredy Kurniawan[3], Yosua Anjupaian Situmeang[1], Yunita Triana[1]

[1] *Department of Materials and Metallurgical Engineering, Kalimantan Institute of Technology, Balikpapan, 76127, Indonesia*
[2] *Mechanical Engineering Department, Kalimantan Institute of Technology, Balikpapan, 76127, Indonesia.*
[3] *Department of Chemistry, Faculty of Science, Kalimantan Institute of Technology, Balikpapan, 76127, Indonesia.*

Corresponding Authors E-mail: hizkia.ad@lecturer.itk.ac.id

Article Info

Article info:
Received: 09-12-2025
Revised: 04-05-2026
Accepted: 24-05-2026

Keywords:
CoO NPs, Green, Cobalt, Synthesis.

How To Cite:
H. A. Dewanto, S. Toding, I. Riadin, J. Awali, A. I. Ismail, F. Kurniawan, Y. A. Situmeang, and Y. Triana, "Characterization of Green-Synthesized Cobalt Oxide Nanoparticles Using Nigella sativa Seed Extract", Indonesian Physical Review, vol. 9, no. 2, p 398-412, 2026.

DOI:
https://doi.org/10.29303/ipr.v9i2.630.

Abstract

Cobalt oxide nanoparticles (CoO NPs) were synthesized via green synthesis using Nigella sativa seed extract as a natural reducing and stabilizing agent. This approach enables environmentally friendly production of ultrafine nanoparticles while incorporating bioactive plant compounds. The CoO NPs were characterized using XRD, XRF, UV–Vis, FTIR, and TEM. XRD confirmed CoO formation with diffraction peaks at 2θ = 31.247°, 36.712°, 42.5°, 44.771°, 59.359°, 61.536°, 65.227°, 74.31°, and 76.111°, which are indexed to the (100), (111), (200), (102), (110), (103), (220), (311), and (222) planes of face-centered cubic (fcc) CoO. XRF showed cobalt as the main element (71.36 wt%) with minor P, S, K, Ca, Fe, Zn, Cu, Mn, and Ti. UV–Vis exhibited peaks at 320 nm and 344 nm, TEM revealed nearly spherical particles (1.72 nm with a standard deviation of 0.55 nm), and FTIR confirmed Co–O bonds (700–663 cm $^{-1}$) along with organic functional groups from the extract. The formation mechanism involves phytochemical-mediated bioreduction, surface stabilization, and producing well-dispersed CoO NPs. Overall, all characterization techniques consistently confirm the successful formation of highly crystalline, pure, and well-dispersed CoO nanoparticles with nanoscale dimensions. The combined results demonstrate that Nigella sativa extract effectively acts as both reducing and stabilizing agent, leading to stable CoO NPs suitable for potential applications in catalytic and functional material systems.

Introduction

Nanotechnology has emerged as a transformative research field over the past few decades, enabling precise manipulation of materials at the nanoscale and yielding unique physical, chemical, and biological properties [1]. Among various nanomaterials, cobalt oxide nanoparticles (CoO NPs) have attracted significant attention due to their remarkable catalytic activity [2],

magnetic properties [3], high electrical conductivity [4], and antimicrobial effects [5]. These properties make CoO NPs highly promising for applications in energy storage, electronics, catalysis, and biomedical devices [6]. Despite their great potential, conventional synthesis methods such as hydrothermal synthesis, chemical precipitation, sol–gel, and chemical wet methods often involve hazardous chemicals and extreme reaction conditions, posing risks to both the environment and human health [7, 8].

Green synthesis has gained recognition as a sustainable and environmentally friendly alternative for nanoparticle production [9]. This approach utilizes phytochemicals derived from plant extracts as natural reducing and stabilizing agents [10], eliminating the need for toxic reagents while offering precise control over particle size, shape, and morphology [11]. In addition, green synthesis is cost-effective, safer for both humans and the environment, and allows the incorporation of the plant's bioactive properties into the nanoparticles, enhancing their functional performance [12]. Previous studies have successfully applied green synthesis to a variety of nanoparticles, including zinc oxide nanoparticles [13] and silver nanoparticles [14] *Nigella sativa* seed extract.

Nigella sativa seed, commonly known as black cumin seed, is a medicinal plant rich in bioactive compounds such as thymoquinone, flavonoids, and phenolics [15]. These phytochemicals act as efficient reducing agents for metal ions and simultaneously serve as capping molecules, stabilizing the formed nanoparticles and preventing excessive growth and aggregation. Moreover, the strong antioxidant properties of black cumin seed extract facilitate the formation of stable and ultrafine CoO NPs [16]. Incorporating these natural compounds into nanoparticle synthesis not only promotes environmentally friendly practices but also imparts the biological functionality of the plant into the final nanomaterial, enhancing its overall performance and potential applications.

Although green synthesis of CoO nanoparticles (CoO NPs) has been widely reported due to its environmental friendliness and simplicity, previous studies still show limitations in comprehensive characterization. Most reports focus mainly on synthesis confirmation and basic structural analysis, while detailed evaluation of particle size distribution, morphology, surface chemistry, and optical properties is often limited or not fully correlated with the role of phytochemical constituents. In particular, the interaction between plant-derived bioactive compounds and their influence on nanoparticle formation, stabilization, and surface functionalization remains insufficiently understood. Therefore, this study aims to address these gaps by employing Nigella sativa seed extract as a plant-mediated reducing and capping agent, with comprehensive characterization using UV–Vis, XRD, FTIR, XRF, and TEM to systematically evaluate the physicochemical properties, structure material, morphology, composition, and optical behavior of the synthesized CoO NPs.

Experimental Method

Black cumin (Nigella sativa) seed extract was used as a reducing agent, while cobalt(II) nitrate hexahydrate ($Co(NO_3)_2 \cdot 6H_2O$) (Merck, analytical grade) served as the precursor. The extract was prepared by heating 5 g of crushed seeds in 100 mL of distilled water at 80 °C for 30 min. Cobalt nitrate (0.2 M) was then added to the extract in a fixed precursor-to-extract ratio of 1:1 (v/v), which was selected to ensure sufficient availability of phytochemical reducing and capping agents to fully interact with Co^{2+} ions, thereby promoting effective reduction and stabilization of the formed nanoparticles. The mixture was stirred at 80 °C for 30 min, followed by aging at room temperature for 24 h. The precipitate was collected by filtration, dried at 80 °C for 10 h,

and identified as CoO nanoparticles (CoO NPs). Characterization was carried out using X-ray fluorescence (XRF), X-ray diffraction (XRD), ultraviolet–visible spectroscopy (UV–Vis), transmission electron microscopy (TEM), and Fourier-transform infrared spectroscopy (FTIR).

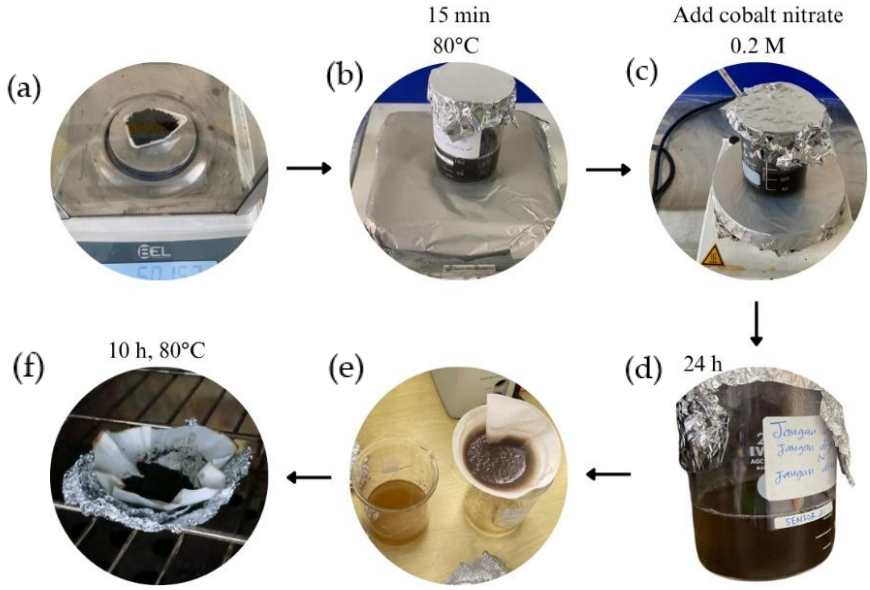

Figure 1. Schematic synthesis of CoO nanoparticles (CoO NPs) using *Nigella sativa* extract, (a) extraction, (a) heating, (c) precursor addition, (d) aging, (e) filtration, and (f) drying processes.

The physicochemical properties of CoO NPs were characterized using X-ray fluorescence (XRF, ED-XRF Horiba Scientific MESA-50), X-ray diffraction (XRD, Bruker D8 Advance, Cu Kα radiation, λ = 1.5406 Å, current 30 mA, and 2θ = 20-80°), ultraviolet–visible spectroscopy (UV–Vis, Orion AquaMate 6100, 190–1100 nm), Fourier-transform infrared spectroscopy (FTIR, Bruker Alpha II, 600–4000 cm^{-1}, ATR ZnSe), and transmission electron microscopy (TEM, HT7700). Elemental composition, crystal structure, optical properties, functional groups, and morphology with particle size distribution were analyzed accordingly. All data were collected as spectra and micrographs and interpreted descriptively, with comparison to relevant literature to evaluate the synthesis efficiency and nanoparticle quality.

Result and Discussion

The characterization of cobalt oxide nanoparticles (CoO NPs) synthesized via a green route using *Nigella sativa* seed extract was performed to elucidate their elemental composition, crystal structure, optical properties, functional groups, and morphological characteristics. The green synthesis approach employing plant extract plays a critical role in nanoparticle formation through phytochemical-mediated reduction and stabilization processes. The characterization techniques applied in this study included X-ray fluorescence (XRF), X-ray diffraction (XRD), ultraviolet–visible spectroscopy (UV–Vis), transmission electron microscopy (TEM), and Fourier-transform infrared spectroscopy (FTIR), as presented in Figures 2–5.

XRF Analysis

Based on Figure 2, the XRF spectrum exhibits a dominant peak at approximately 6.9 keV with an intensity exceeding 30,000 counts, corresponding to the characteristic Kα emission of cobalt (Co). This result confirms that cobalt is the primary elemental constituent of the synthesized nanoparticles. The high intensity of the cobalt peak indicates that Co^{2+} ions derived from the cobalt nitrate precursor were successfully incorporated into the nanoparticle structure through a reduction process facilitated by phytochemical compounds present in the Nigella sativa seed extract. To further support this observation, the quantitative elemental composition obtained from XRF analysis is presented in Table 1, demonstrating that cobalt possesses the highest weight percentage among the detected elements. The high cobalt content further suggests that Co is the dominant metallic species in the system, which is consistent with the formation of CoO as the main phase as confirmed by XRD analysis.

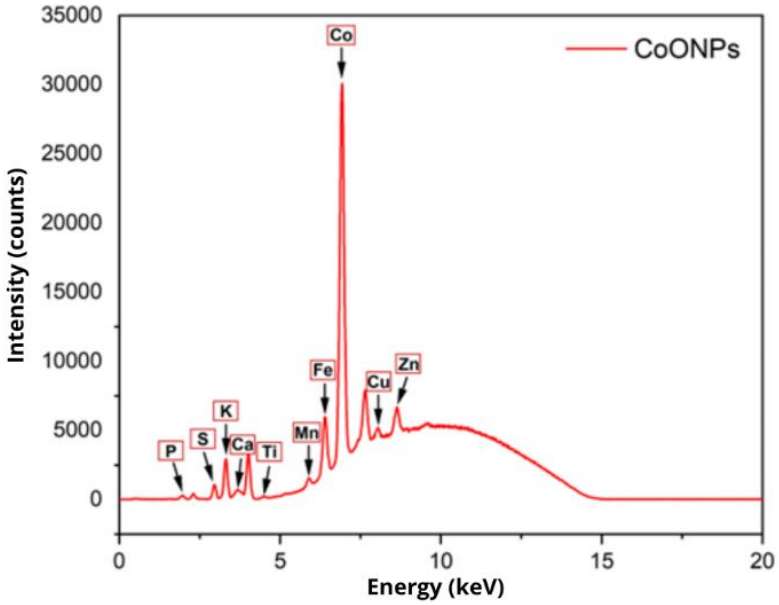

Figure 2. X-ray fluorescence (XRF) spectrum of CoO nanoparticles (CoO NPs)

In addition to cobalt, several minor elemental signals were detected, including phosphorus (P), sulphur (S), potassium (K), calcium (Ca), titanium (Ti), manganese (Mn), iron (Fe), copper (Cu), and zinc (Zn) [9]. These elements originate from the natural mineral content of *Nigella sativa* seeds and are commonly observed in plant-mediated synthesis routes [17]. Their relatively low concentrations, as summarized in Table 1, indicate that they function as trace elements associated with the plant extract rather than contributing to the formation of unwanted crystalline impurities. Therefore, the XRF results confirm the elemental dominance of cobalt while reflecting the complex biochemical composition of the green synthesis system.

Table 1. XRF-derived elemental composition of CoO NPs

Elements	Concentration (wt%)	X-ray Line	Intensity
Co	71.36	Kα	31059.29
K	8.77	Kα	1651.32
S	6.21	Kα	167.76
Ca	4.87	Kα	124.38
Fe	3.34	Kα	2788.14
P	2.97	Kα	27.21
Zn	1.30	Kα	1162.19
Cu	0.46	Kα	415.95
Mn	0.40	Kα	292.89
Ti	0.29	Kα	76.59

UV–Visible Spectroscopy Analysis

UV–Visible spectroscopy was employed to investigate the optical properties and electronic transitions associated with the synthesized CoO nanoparticles (CoO NPs) [18]. Nigella sativa seed extract contains various bioactive compounds, including flavonoids, phenolic compounds, and quinone derivatives [19], which can act as reducing and capping agents during the synthesis process. These molecules possess oxygen-containing functional groups, such as carbonyl (C=O) and aromatic C=C groups, which are commonly involved in metal–ligand interactions and surface coordination [20, 21].

The UV–Vis spectrum of the CoO NPs shows absorption features at approximately 320 nm and 344 nm. To better understand these features, the spectrum should be considered in comparison with the corresponding plant extract. In general, the observed absorption bands may be associated with electronic transitions originating from both the organic phytochemicals in the extract and their interaction with cobalt species during nanoparticle formation. The absorption band around 320 nm can be related to π–π* transitions of aromatic systems and n–π* transitions of carbonyl-containing compounds present in the plant extract, which may also participate in coordination with metal ions [22]. The broad feature around 344 nm may be attributed to surface-related electronic states and possible interactions between cobalt species and capping molecules adsorbed on the nanoparticle surface.

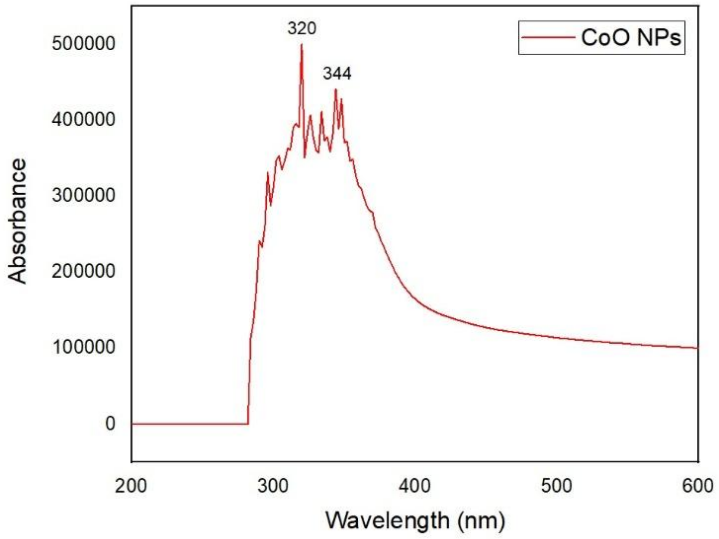

Figure 3. UV–Vis spectra of CoO nanoparticles (CoO NPs)

The absorption peaks observed at 320 nm and 344 nm in Figure 3 are consistent with literature reports on CoO nanoparticles interacting with organic ligands (phenolic and flavonoid), where characteristic absorption bands are typically found in the ranges of 337–345 nm and 343–360 nm [23]. This agreement indicates that the UV–Vis spectral features obtained in this study are consistent with the optical properties of organically stabilized CoO nanoparticles, thereby confirming the successful green synthesis of CoO NPs using Nigella sativa seed extract.

XRD Analysis

X-ray diffraction (XRD) analysis was conducted to investigate the crystal structure and phase composition of the synthesized cobalt oxide nanoparticles (CoO NPs). The diffraction pattern, as shown in Figure 4, exhibits distinct peaks at 2θ = 31.247°, 36.712°, 42.5°, 44.771°, 59.359°, 61.536°, 65.227°, 74.31°, and 76.111°, which are indexed to the (100), (111), (200), (102), (110), (103), (220), (311), and (222) planes of face-centered cubic (fcc) CoO, in good agreement with JCPDS card No. 96-152-8839 [24-26], confirming the formation of crystalline CoO nanoparticles. The crystallite size was estimated using the Scherrer (Eq. 1):

$$D = \frac{K\lambda}{\beta \cos\theta} \quad (1)$$

where K is the shape factor (0.9), λ is the X-ray wavelength (1.5406 Å), β is the full width at half maximum (FWHM), and θ is the Bragg angle [27]. The average crystallite size obtained was 0.938 nm, indicating the formation of highly confined crystalline domains with significant surface contribution, which is beneficial for electrochemical applications.

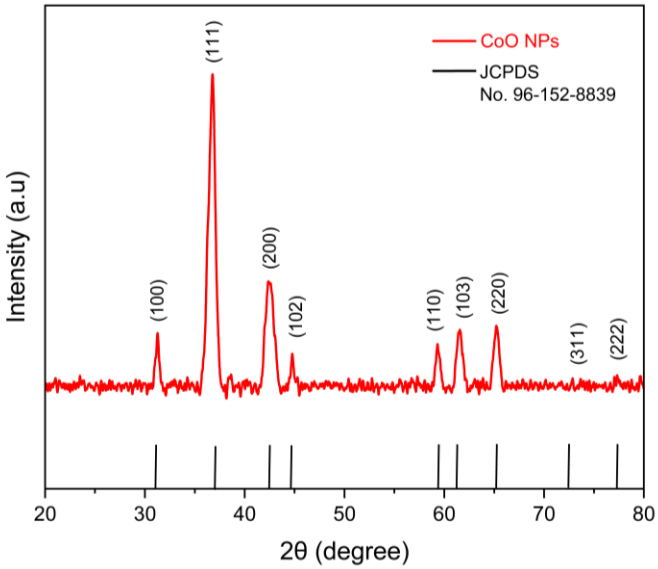

Figure 4. X-ray diffraction (XRD) diffractogram of cobalt nanoparticles (CoO NPs)

To further elucidate the crystallographic properties of the synthesized CoO NPs, structural parameters including lattice constant (a), unit cell volume (V_{cell}), and theoretical X-ray density (ρ_{XRD}) were determined based on the rock-salt (NaCl-type, fcc) structure of CoO, consistent with the indexed diffraction pattern. The interplanar spacing (d) was calculated using Bragg's law (Eq. 2) and subsequently used to determine the lattice parameter through the standard cubic relationship.

$$n\lambda = 2d \sin\theta \tag{2}$$

where λ = 1.5406 Å and n = 1 [28]. The obtained d-values were then used to determine the lattice parameter using the cubic relation:

$$a = d\sqrt{h^2 + k^2 + l^2} \tag{3}$$

The average lattice parameter was calculated to be 4.29 Å, slightly higher than the literature values of 4.2676 Å and 4.258 Å, as reported by [29] and [30]. This deviation is likely related to the reduced crystallite size of the synthesized nanoparticles, which induces lattice distortion due to enhanced surface effects, and may also be influenced by possible lattice strain and defect formation, including oxygen vacancies, generated during the rapid nucleation process under green synthesis conditions [31, 32]. The unit cell volume for the cubic system was calculated using (Eq. 4):

$$V_{cell} = a^3 \tag{4}$$

resulting in a value of 79.01 Å^3. The theoretical X-ray density was determined using (Eq. 5):

$$\rho_{XRD} = \frac{Z \cdot M}{N_A \cdot V_{cell}} \tag{5}$$

The theoretical X-ray density was calculated using $Z = 4$ for the rock-salt (NaCl-type) fcc structure, $M\ (CoO) = 74.93\ g\ mol^{-1}$, and $N_A = 6.022 \times 10^{23}\ mol^{-1}$[33]. The obtained density was 6.3 g/cm^3, which is slightly lower than the value reported in the Materials Project database for cubic CoO (space group $Fm\bar{3}m$, mp-19079), i.e., 6.5 g/cm^3. This deviation is likely attributed to nanoscale effects in the synthesized material, where reduced crystallite size increases the surface-to-volume ratio and surface energy contribution, and may also induce lattice distortion and defect formation, leading to an apparent modification of the X-ray density, as commonly observed in nanosized transition metal oxides synthesized via green routes [34].

Overall, the XRD results confirm that the synthesized CoO NPs predominantly crystallize in a well-defined fcc CoO phase. The slight variations in lattice parameter, unit cell volume, and X-ray density, together with the presence of a weak secondary diffraction feature, further support the influence of nanoscale effects and defect formation induced by the green synthesis approach.

Table 2. Structural parameters and theoretical XRD density of CoO nanoparticles (CoO NPs)

D (nm)	a (Å)	v_{cell} (Å^3)	v_{cell} (cm^3)	ρ_{xrd} (g cm^{-3})
0.938	4.29	79.01	7.901×10^{-23}	6.30

TEM Analysis

The morphological characteristics of the synthesized CoO nanoparticles (CoO NPs) were examined using TEM at a magnification of 60,000× and an accelerating voltage of 120 kV. The TEM images reveal that the nanoparticles are nearly spherical in shape and relatively uniformly distributed, although slight agglomeration is observed. The agglomeration is commonly reported for metal oxide nanoparticles due to their high surface energy [35]. Particle size analysis indicates that the CoO NPs have diameters below 5 nm, with an average particle size of 1.72 nm and a standard deviation of 0.55 nm. The particle size distribution histogram shows that most nanoparticles fall within the 1–3 nm range, with a dominant population around 1.5–2.0 nm, indicating effective control over nucleation and growth during the synthesis process.

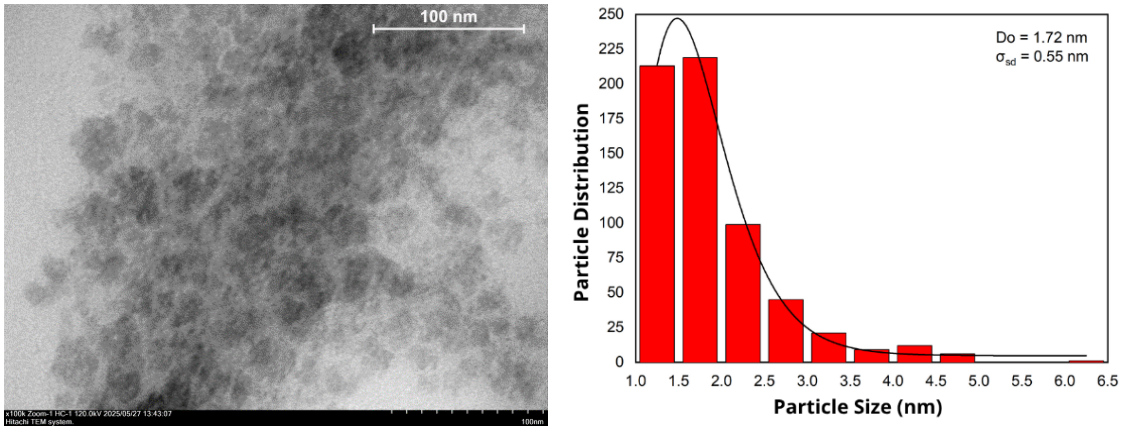

(a) (b)

Figure 5. (a) TEM image of cobalt oxide nanoparticles (CoO NPs) and (b) corresponding particle size distribution histogram

A comparison of the average particle size obtained in this study with previously reported CoO nanoparticles is presented in Table 2. reported CoO nanoparticles with an average size of 65.4 nm [36], while [37] and [38] reported smaller particle sizes of 14.4 nm and 10 nm, respectively. Notably, the CoO NPs synthesized in this study exhibit a significantly smaller average particle size, highlighting the effectiveness of the green synthesis approach using *Nigella sativa* seed extract. The presence of phytochemical compounds acting simultaneously as reducing and capping agents plays a crucial role in suppressing particle growth and preventing excessive aggregation, resulting in ultrafine nanoparticles. The ultrafine particle size obtained in this study implies a high specific surface area, which is highly desirable for various functional material applications, including catalysis, sensing, and electrochemical devices [39, 40].

Table 3. Comparison of average particle size of CoO NPs obtained from different studies

Synthesis Methods	Average Particle Size (nm)	Ref.
Chemical method	65.4	[36]
Chemical/solution-based method	14.4	[37]
Modified chemical synthesis	10.0	[38]
Green synthesis-based *Nigella sativa* seed extract	1.72	This study

FTIR Analysis

FTIR spectroscopy was employed to identify the surface functional groups of the synthesized cobalt oxide nanoparticles (CoO NPs) and to confirm the formation of Co–O metal–oxygen bonds. As presented in Table 4 and Figure 6, the FTIR spectrum exhibits characteristic absorption bands corresponding to both residual organic moieties and inorganic metal–oxygen vibrations. The absorption bands observed at 2921 cm^{-1} and 2851 cm^{-1} were assigned to the asymmetric and symmetric stretching vibrations (ν_{as} and ν_s) of aliphatic -CH_2 and -CH_3 groups, indicating the presence of residual phytochemical compounds such as alcohols and hydrocarbons derived from *Nigella sativa* extract [41]. The band at 1708 cm^{-1} corresponds to C=O stretching vibration (ν(C=O)), typically associated with carbonyl groups in flavonoids, fatty acids, and quinone derivatives [42]. Meanwhile, the peak at 1020 cm^{-1} is attributed to C-O stretching vibration (ν(C–O)), confirming oxygen-containing organic species on the nanoparticle surface [43]. Importantly, the absorption bands at 700 cm^{-1} and 663 cm^{-1} are attributed to metal-oxygen stretching vibrations (ν_1 and ν_2 modes) of Co-O bonds within the cobalt oxide lattice [23]. These two distinct vibrational modes are characteristic of Co-O bonding in cobalt oxide systems and confirm the successful formation of crystalline CoO nanoparticles.

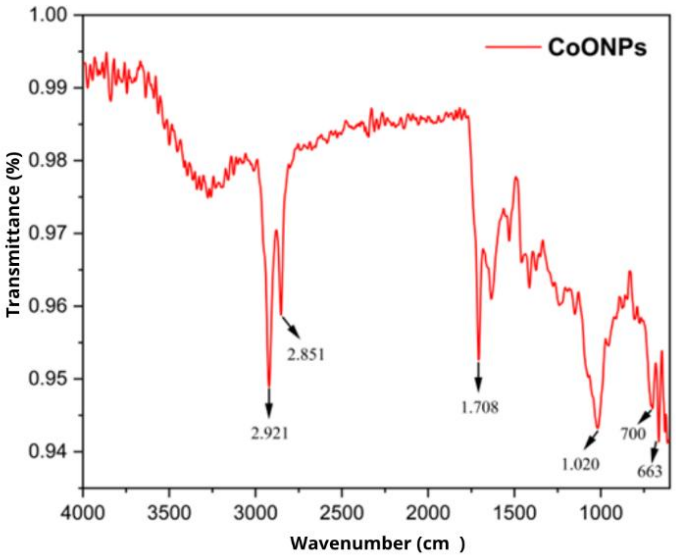

Figure 6. FTIR spectrum of cobalt oxide nanoparticles (CoO NPs)

The coexistence of organic functional groups and Co–O vibrational modes suggests that phytochemical constituents act as both reducing and capping agents, thereby enhancing nanoparticle stability and dispersion. In particular, flavonoids, phenolic compounds, fatty acids, and quinone derivatives from the *Nigella sativa* extract are likely responsible for surface coordination and capping of the nanoparticles. Minor shifts in peak positions compared to literature values may be attributed to particle size effects, surface coordination with these organic ligands, and morphological variations, further supporting the successful plant extract-mediated reduction of stabilized CoO NPs [26, [4].

Table 4. Functional groups in the FTIR spectrum of CoO NPs

Wavenumber (cm^{-1})	Vibrational Mode	Functional Group	Assignment
2921	ν_{as} (C–H)	$-CH_2$ / $-CH_3$	Asymmetric stretching of aliphatic hydrocarbons
2851	ν_s (C–H)	$-CH_2$ / $-CH_3$	Symmetric stretching of aliphatic hydrocarbons
1708	ν(C=O)	Carbonyl group	Flavonoids, fatty acids, quinone derivatives
1020	ν(C–O)	C-O bond	Oxygen-containing organic compounds
700	ν_1 (Co-O)	Metal–oxygen bond	Co–O lattice vibration
663	V2 (Co-O)	Metal–oxygen bond	Co–O lattice vibration

Proposed Formation Mechanism of CoO NPs

The formation of CoO nanoparticles using *Nigella sativa* seed extract occurs through an eco-friendly plant extract-mediated reduction and stabilization mechanism, in which phytochemicals such as flavonoids, phenolic compounds, quinone derivatives, and fatty acids act as natural reducing and capping agents. Co^{2+} ions from cobalt nitrate are initially reduced to highly reactive Co^0 species, which serve as nucleation sites for particle formation and subsequently aggregate to form cobalt clusters [45]. Simultaneously, the adsorption of organic molecules on the particle surface limits excessive growth and prevents agglomeration, yielding nanoparticles with controlled size. Controlled oxidation of these Co^0 species, under mild thermal treatment and exposure to ambient oxygen, ultimately produces stable CoO nanoparticles, demonstrating an efficient and environmentally friendly synthesis route without the need for hazardous chemical reducing agents.

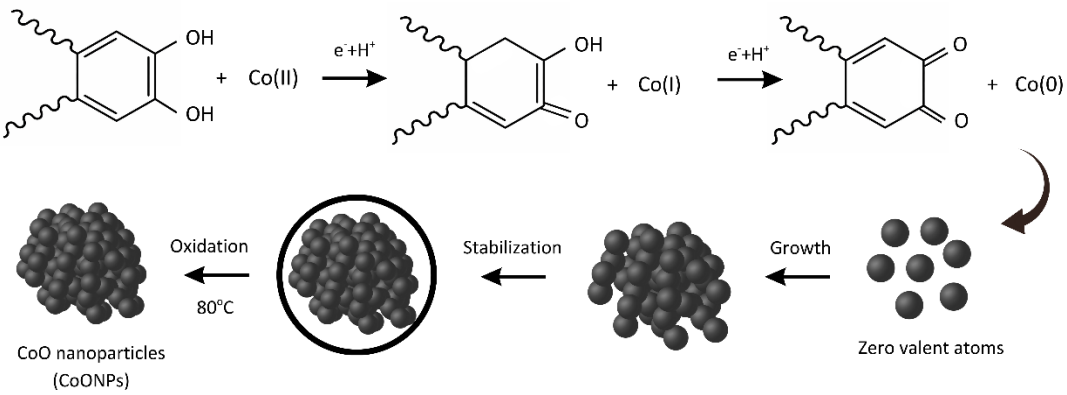

Figure 7. Proposed mechanism for the plant extract-mediated reduction and stabilization of CoO nanoparticles mediated by *Nigella sativa* seed extract

Conclusion

Cobalt oxide nanoparticles (CoO NPs) were successfully synthesized via a green approach using *Nigella sativa* seed extract as a natural reducing and capping agent. XRF analysis confirmed cobalt as the dominant element (71.36 wt%), while TEM images revealed nearly spherical nanoparticles with an average size of 1.72 nm and a narrow size distribution. XRD patterns indicated a well-defined CoO phase structure, and UV–Vis spectra showed characteristic absorption peaks at 320 nm and 344 nm, corresponding to ligand-to-metal charge transfer and surface electronic transitions influenced by organic capping molecules. FTIR analysis confirmed the presence of organic functional groups from the extract (C=O and C–O) and Co–O bonds, demonstrating that phytochemicals effectively stabilized and capped the nanoparticles. The proposed formation mechanism involves Co^{2+} reduction to Co^0 species, nucleation and cluster growth, surface capping by phytochemicals, and controlled oxidation to form stable CoO nanoparticles. Overall, the results indicate that green synthesis using *Nigella sativa* produces ultrafine, and stable CoO NPs with desirable physicochemical properties, providing an eco-friendly route suitable for applications in catalysis, electronics, and biomedical fields.

Acknowledgment

This work is supported by research funding from BIMA Kemdiktisaintek 2024–2025 by the Ministry of Education, Technology, and Innovation. The authors also express their sincere gratitude to the Institute for Research and Community Service (LPPM) of Institut Teknologi Kalimantan for the support and facilitation provided throughout this study.

References

[1] B. Boddeda, B. Erothi, and S. Putta, "Nanofabrication: Advances, Applications, and Future Prospects In Emerging Technologies," *Biosci. Biotechnol. Res. Asia*, vol. 4, no. 22, p. 1294, Dec. 2025.

[2] D. A. Kader, "Green synthesis of cobalt oxide nanoparticles (Co3O4NPs): Characterization and green light-driven photocatalytic aerobic oxidation of alkyl and aryl sulfides to the corresponding sulfoxides," *Materials Today Sustainability*, vol. 28, p. 100997, Dec. 2024.

[3] A. A. Vodyashkin, P. Kezimana, F. Y. Prokonov, I. A. Vasilenko, and Y. M. Stanishevskiy, "Current Methods for Synthesis and Potential Applications of Cobalt Nanoparticles: A Review," *Crystals (Basel).*, vol. 12, no. 2, p. 272, Feb. 2022.

[4] J. Iqbal *et al.*, "Cobalt Oxide Nanograins and Silver Nanoparticles Decorated Fibrous Polyaniline Nanocomposite as Battery-Type Electrode for High Performance Supercapattery," *Polymers (Basel).*, vol. 12, no. 12, p. 2816, Nov. 2020.

[5] A. Waris *et al.*, "Green fabrication of Co and Co $_3$ O $_4$ nanoparticles and their biomedical applications: A review," *Open Life Sci.*, vol. 16, no. 1, pp. 14–30, Jan. 2021.

[6] E. Papis *et al.*, "Engineered cobalt oxide nanoparticles readily enter cells," *Toxicol. Lett.*, vol. 189, no. 3, pp. 253–259, Sep. 2009.

[7] H. M. Abuzeid, C. M. Julien, L. Zhu, and A. M. Hashem, "Green Synthesis of Nanoparticles and Their Energy Storage, Environmental, and Biomedical Applications," *Crystals (Basel).*, vol. 13, no. 11, p. 1576, Nov. 2023.

[8] M. N. Subramaniam, P. S. Goh, W. J. Lau, and A. F. Ismail, "The Roles of Nanomaterials in Conventional and Emerging Technologies for Heavy Metal Removal: A State-of-the-Art Review," *Nanomaterials*, vol. 9, no. 4, p. 625, Apr. 2019.

[9] L. P. V. Silva *et al.*, "On the road to sustainability – application of metallic nanoparticles obtained by green synthesis in dentistry: a scoping review," *Beilstein Journal of Nanotechnology*, vol. 16, pp. 1851–1862, Oct. 2025.

[10] S. Bawazeer, "Green Synthesis: An Eco-Friendly Approach for the Synthesis of Silver Nanoparticles Functionalized with Operculina turpethum and It's In vitro and in vivo Biological Activities," *Int. J. Nanomedicine*, vol. Volume 20, pp. 2991–3005, Mar. 2025.

[11] G. I. Edo *et al.*, "Eco-friendly nanoparticle phytosynthesis via plant extracts: Mechanistic insights, recent advances, and multifaceted uses," *Nano TransMed*, vol. 4, p. 100080, Dec. 2025.

[12] S. Singaravelu, F. Motsoene, H. Abrahamse, and S. S. Dhilip Kumar, "Green-synthesized metal nanoparticles: a promising approach for accelerated wound healing," *Front. Bioeng. Biotechnol.*, vol. 13, Jul. 2025.

[13] S. Waseem *et al.*, "Green Synthesis of ZnO nanoparticles using Nigella sativa seed extract for antibacterial activities," *Nano-Structures & Nano-Objects*, vol. 38, p. 101212, May 2024.

[14] J. Ferdous *et al.*, "Green synthesis and characterization of silver nanoparticles from Nigella sativa L seeds and It's against human pathogenic bacteria and fungi," *The Microbe*, vol. 4, p. 100111, Sep. 2024.

[15] M. H. Alu'datt *et al.*, "Designing novel industrial and functional foods using the bioactive compounds from *Nigella sativa* L. (black cumin): Biochemical and biological prospects toward health implications," *J. Food Sci.*, vol. 89, no. 4, pp. 1865–1893, Apr. 2024.

[16] R. Shanmugam, M. Tharani, S. S. Abullais, S. R. Patil, and M. I. Karobari, "Black seed assisted synthesis, characterization, free radical scavenging, antimicrobial and anti-inflammatory activity of iron oxide nanoparticles," *BMC Complement. Med. Ther.*, vol. 24, no. 1, p. 241, Jun. 2024.

[17] B. Beyzanur, R. Péter, and C. Furkan, "Evaluation of the Chemical Composition of Nigella sativa L. Seeds Grown in Different Locations," *Research Article Araştırma Makalesi*, vol. 57, no. 1, pp. 11–18, 2025.

[18] Y. Sang, H. Liu, and A. Umar, "Photocatalysis from UV/Vis to Near-Infrared Light: Towards Full Solar-Light Spectrum Activity," *ChemCatChem*, vol. 7, no. 4, pp. 559–573, Feb. 2015.

[19] A. Mengesha Yessuf, "Phytochemical Extraction and Screening of Bio Active Compounds from Black Cumin (Nigella Sativa) Seeds Extract," *American Journal of Life Sciences*, vol. 3, no. 5, p. 358, 2015.

[20] P. K. Walencik, R. Choińska, E. Gołębiewska, and M. Kalinowska, "Metal–Flavonoid Interactions—From Simple Complexes to Advanced Systems," *Molecules*, vol. 29, no. 11, p. 2573, May 2024.

[21] Y. Bao, W. An, C. H. Turner, and K. M. Krishnan, "The Critical Role of Surfactants in the Growth of Cobalt Nanoparticles," *Langmuir*, vol. 26, no. 1, pp. 478–483, Jan. 2010.

[22] M. Sisa, S. L. Bonnet, D. Ferreira, and J. H. Van der Westhuizen, "Photochemistry of Flavonoids," *Molecules*, vol. 15, no. 8, pp. 5196–5245, Aug. 2010.

[23] Y. Shinde, "Green Synthesis and Characterisation of Iron and Cobalt Oxide Nanoparticles Using Piper Dravidii Leaves Extract," *International Journal of Scientific Research and Engineering Trends*, vol. 11, no. 1, pp. 843–848, Jan. 2025.

[24] S. V. Santos *et al.*, "Synthesis and Local Characterization of CoO Nanoparticles in Distinct Phases: Unveiling Polymorphic Structures," *ACS Omega*, vol. 9, no. 42, pp. 42883–42894, Oct. 2024.

[25] X. Q. Zhao, S. Veintemillas-Verdaguer, O. Bomati-Miguel, M. P. Morales, and H. B. Xu, "Thermal history dependence of the crystal structure of Co fine particles," *Phys. Rev. B*, vol. 71, no. 2, p. 024106, Jan. 2005.

[26] S. Sheikh *et al.*, "Sustainable plant mediated synthesis of cobalt oxide nanoparticles using Uraria picta extract with enhanced biological activity," *Sci. Rep.*, vol. 15, no. 1, p. 44017, Dec. 2025.

[27] M. Faraji, Y. Yamini, and N. Salehi, "Characterization of magnetic nanomaterials," in *Magnetic Nanomaterials in Analytical Chemistry*, Elsevier, pp. 39–60, 2021.

[28] P. R. Bhattacharjee, "Discovery of the lack of success of Bragg's law in respect of perfect quantification of the X-ray diffraction phenomenon," *Next Research*, vol. 2, no. 2, p. 100312, Jun. 2025.

[29] R. Santos *et al.*, "Crystalline and magnetic properties of CoO nanoparticles locally investigated by using radioactive indium tracer," Jul. 08, 2021.

[30] M. Ghosh, E. V. Sampathkumaran, and C. N. R. Rao, "Synthesis and Magnetic Properties of CoO Nanoparticles," *Chemistry of Materials*, vol. 17, no. 9, pp. 2348–2352, May 2005

[31] A. Kalita and M. P. C. Kalita, "Size dependence of lattice parameters in ZnO nanocrystals," *Applied Physics A*, vol. 121, no. 2, pp. 521–524, Nov. 2015.

[32] S. Deshpande, S. Patil, S. V. Kuchibhatla, and S. Seal, "Size dependency variation in lattice parameter and valency states in nanocrystalline cerium oxide," *Appl. Phys. Lett.*, vol. 87, no. 13, p. 133113, Sep. 2005.

[33] W.-B. He, J.-L. Fan, Q. Zhang, Y. Jin, W. Yuan, and Q.-W. Zhang, "Thin layer identification using a theoretical X-ray logging while drilling (LWD) density imaging tool," *Pet. Sci.*, vol. 22, no. 6, pp. 2403–2413, Jun. 2025.

[34] A. Chen, Q. Su, H. Han, E. Enriquez, and Q. Jia, "Metal Oxide Nanocomposites: A Perspective from Strain, Defect, and Interface," *Advanced Materials*, vol. 31, no. 4, Jan. 2019.

[35] A. A. Belew and M. A. Assege, "Solvothermal synthesis of metal oxide nanoparticles: A review of applications, challenges, and future perspectives," *Results Chem.*, vol. 16, p. 102438, Jul. 2025.

[36] J. Jeong, Y. Han, C. A. Poland, and W.-S. Cho, "Response-metrics for acute lung inflammation pattern by cobalt-based nanoparticles," *Part. Fibre Toxicol.*, vol. 12, no. 1, p. 13, Dec. 2015.

[37] H. Zhang, L. V. Solomon, D.-H. Ha, S. Honrao, R. G. Hennig, and R. D. Robinson, "(NH4)2S, a highly reactive molecular precursor for low temperature anion exchange reactions in nanoparticles," *Dalton Transactions*, vol. 42, no. 35, p. 12596, 2013.

[38] X. Chen, H. van Gog, and M. A. van Huis, "Transformation of Co_3O_4 nanoparticles to CoO monitored by *in situ* TEM and predicted ferromagnetism at the Co_3O_4/CoO interface from first principles," *J. Mater. Chem. C Mater.*, vol. 9, no. 17, pp. 5662–5675, 2021.

[39] E. E. Abdel-Hady, M. Shaban, M. O. Abdel-Hamed, A. Gamal, H. Yehia, and A. M. Ahmed, "Synthesis and Characterization of NiCoPt/CNFs Nanoparticles as an Effective Electrocatalyst for Energy Applications," *Nanomaterials*, vol. 12, no. 3, p. 492, Jan. 2022.

[40] W. Wei, J. Xu, W. Chen, L. Mi, and J. Zhang, "A review of sodium chloride-based electrolytes and materials for electrochemical energy technology," *J. Mater. Chem. A Mater.*, vol. 10, no. 6, pp. 2637–2671, 2022.

[41] K. Bixapathi, G. Prabhakar, and P. Kamalakar, "Preliminary Phytochemical Screening, Quantification, and Identification of Active Compounds in Acalypha malabarica Müll.Arg Using FTIR and GC-MS Analysis," *Plant Science Archives*, pp. 30–40, Nov. 2024.

[42] M. C. Celina, E. Linde, and E. Martinez, "Carbonyl Identification and Quantification Uncertainties for Oxidative Polymer Degradation," *Polym. Degrad. Stab.*, vol. 188, p. 109550, Jun. 2021.

[43] B. Özkahraman and Z. Özbaş, "Removal of Al(III) Ions Using Gellan Gum-Acrylic Acid Double Network Hydrogel," *J. Polym. Environ.*, vol. 28, no. 2, pp. 689–698, Feb. 2020.

[44] S. V. Santos *et al.*, "Synthesis and Local Characterization of CoO Nanoparticles in Distinct Phases: Unveiling Polymorphic Structures," *ACS Omega*, vol. 9, no. 42, pp. 42883–42894, Oct. 2024.

[45] K. Deka *et al.*, "Understanding the mechanism underlying the green synthesis of metallic nanoparticles using plant extract(s) with special reference to Silver, Gold, Copper and Zinc oxide nanoparticles," *Hybrid Advances*, vol. 9, p. 100399, Jun. 2025.